VIRULENCE
2025, VOL. 16, NO. 1, 2472877
https://doi.org/10.1080/21505594.2025.2472877

Taylor & Francis
Taylor & Francis Group

RESEARCH ARTICLE

OPEN ACCESS Check for updates

UvCYP503 is required for stress response and pathogenicity in *Ustilaginoidea virens*

Xiuxiu Cao [a,b], Hui Wen[a], Dagang Tian[c], Huanbin Shi[a], Kabin Xie[b], Jiehua Qiu [a], and Yanjun Kou [a]

[a]State Key Laboratory of Rice Biology and Breeding, China National Rice Research Institute, Hangzhou, China; [b]National Key Laboratory of Crop Genetic Improvement and National Center of Plant Gene Research (Wuhan), Hubei Hongshan Laboratory, Huazhong Agricultural University, Wuhan, China; [c]Biotechnology Research Institute, Fujian Academy of Agricultural Sciences, Fuzhou, Fujian, China

ABSTRACT

The fungus *Ustilaginoidea virens*, which impacts rice spikes, causes rice false smut (RFS), a significant prevalent disease in rice cultivation regions globally. Cytochrome *P450* genes are known to be involved in secondary metabolism and pathogenesis in various species, but studies on *CYP450* genes in *U. virens* are limited. In this research, a *P450* family gene, *CYP503*, was found up-regulated during invasion stage of *U. virens*. Observation of fluorescence indicated that UvCYP503-GFP is situated within cytoplasm of hyphae. Disruption of *CYP503* led to decreased hyphal development, conidiation, and pathogenicity. Additional RNA-seq assay revealed that *UvCYP503* affects the transcript of genes associated with pathogenicity, various stress responses, and other *CYP450* genes. In alignment with RNA-seq results, compared with wild-type, Δ*Uvcyp503* mutants showed increased sensitivity to cell wall stresses, but reduced sensitivity to osmotic and hyperosmotic stressors. Moreover, Δ*Uvcyp503* mutants exhibited decreased sensitivity to the fungicides difenoconazole and tebuconazole. This study represents a phenome-based functional analysis of a *CYP503* gene in *U. virens* and provides valuable genetic resources for further research in filamentous fungi and other plant pathogens.

ARTICLE HISTORY
Received 29 September 2024
Revised 27 December 2024
Accepted 9 February 2025

KEYWORDS
Rice false smut; virulence; Cytochrome P450; azole fungicides

Introduction

Cytochrome P450 (CYP450) belongs to a superfamily of haem-containing enzymes that are present in a wide range of species, including fungi, bacteria, plants, and animals [1,2]. By adding an oxygen atom obtained from molecular oxygen, CYP450 enzymes play crucial roles in accelerating the transformation of lipophilic substances into more hydrophilic derivatives [3–6]. In *Aspergillus nidulans*, for example, the *phacB* gene encodes enzyme CYP504B is responsible for hydroxylating aromatic rings of phenylacetic acid [7]. Similarly, in *Phanerochaete chrysosporium*, CYP450 enzymes can catalyse the oxidation of phenanthrene under lignin-olytic conditions [8]. Members of the CYP52 family, such as the BbCYP52×1 enzyme in *Beauveria bassiana* and MrCYP52 in *Metarhizium robertsii*, are involved in modifying insect epicuticles to hydrophilic derivatives [9,10]. Pathogens like *Nectria haematococca* can produce the pisatin demethylase (a CYP450 enzyme), which demethylates the pea phytoalexin pisatin, thereby reducing its toxicity to the pathogen [11].

CYP450 enzymes are also crucial for the synthesis of secondary metabolites. In *Fusarium fujikuroi*, four CYP450 genes, namely *P450–1*, *P450–2*, *P450–3*, and *P450–4* mediate ten of the fifteen steps of the gibberellin synthesis pathway [12,13]. In *Artemisia annua* L, CYP71AV1 is essential for the production of antimalarial sesquiterpene lactone artemisinin [14]. Given the importance of CYP450 proteins in various organisms, CYP450 enzymes are targets for many antifungal agents [15]. For instance, ERG11 (CYP51) in many fungi is involved in ergosterol synthesis, which is a target of azole drugs [16]. Mutations at the E483K and P486S positions of the CYP51A locus in *As. clavatus* can confer resistance to azole agents [17]. These examples highlight the diverse roles of CYP450 enzymes in various biological processes, including detoxification, metabolism, and adaptation to environmental challenges. Whether CYP450 enzymes have similar functions in *Ustilaginoidea virens* remains unknown at present.

Some *CYP450* genes are involved in the virulence of pathogenic fungi [18–21]. For instance, the expression of *CYP505* in *F. oxysporum* is induced when infecting lettuce [22]. Disruption of *PlCB5L1* reduces pathogenicity in *Peronophythora litchi* [23]. Similarly, deletion of *CYP*

CONTACT Yanjun Kou kouyanjun@caas.cn; Jiehua Qiu qiujiehua@caas.cn

© 2025 The Author(s). Published by Informa UK Limited, trading as Taylor & Francis Group.
This is an Open Access article distributed under the terms of the Creative Commons Attribution-NonCommercial License (http://creativecommons.org/licenses/by-nc/4.0/), which permits unrestricted non-commercial use, distribution, and reproduction in any medium, provided the original work is properly cited. The terms on which this article has been published allow the posting of the Accepted Manuscript in a repository by the author(s) or with their consent.

genes in *F. graminearum* leads to decreased pathogenicity [24], while knockout of *MoMCP1* in *Magnaporthe oryzae* affects the expression of many pathogenesis-associated genes [25]. Disruption of *VdCYP1* reduces pathogenicity of *Verticillium dahliae* by affecting secondary metabolism [26]. However, the function of *CYP450* genes in pathogenic fungi remains largely unknown.

U. virens is causing a serious disease in China and worldwide [27]. In China, *U. virens* caused an annual yield loss of 2.4 million hectares loss from 2015 to 2017 [28]. India, as the second largest rice producing country, has suffered yield losses ranging from 0.5% to 75% due to *U. virens* damage [29]. Similarly, *U. viren* caused 80–90% yield loss in the Chitwan district of Nepal based on rice variety [30]. This biotrophic fungus forms false smut balls, which replace normal rice grains, leading to substantial economic losses for farmers [31]. Furthermore, *U. virens* is known to produce mycotoxins, such as cyclopeptide ustiloxins and polyketide ustilaginoidins, some of which pose risks to human and animal health [32–34]. Consequently, researchers have increasingly focused on studying RFS disease. In this paper, we investigated the gene *UvCYP503*, which belongs to CYP450 family, and analysed its function in *U. virens*. By disrupting *UvCYP503*, we found that *UvCYP503* is important for growth, conidiation, and virulence. Furthermore, RNA-seq and quantitative real-time PCR (RT-qPCR) analysis demonstrated that *UvCYP503*-regulated transcription is tightly correlated with pathogenesis, stress responses, and transcription of other *CYP450* genes. Additionally, knockout of *UvCYP503* resulted in reduced sensitivity of *U. virens* to azole fungicides.

Results

Identification of CYP503

Based on previous studies, the *UvCYP503* gene in *U. virens* was found to be up-regulated during infection [35]. For further insights into the possible roles of *UvCYP503*, RT-qPCR was employed to assess the expression patterns of *UvCYP503* during *U. virens* infection. Compared to the mycelial stage, the expression of *UvCYP503* is significant up-regulated at 5 days post-inoculation (dpi) (Figure 1a). This implied that *UvCYP503* might play important functions in *U. virens* colonization during the initial infection phases.

Further analysis using the NCBI Conserved Domain Search revealed that UvCYP503 contains a cytochrome P450 domain (NCBI Conserved Domain Search (nih.gov)), belonging to cytochrome P450 family 503 that catalyse a diverse range of oxidative reactions. To investigate whether CYP503 exhibits conservation across different species, we performed a phylogenetic analysis of CYP503 homologues from *U. virens*, *Neurospora crassa*, *Chaetomium globosum*, *As. niger*, *As. flavus*, *Me. brunneum*, *F. fujikuroi*, *F. oxysporum*, *F. graminearum*, *Talaromyces stipitatus*, *Colletotrichum siamense*, and *T. marneffei*. This analysis revealed that CYP503 proteins are conserved across various fungi, with high similarity to those in *F. fujikuroi* and *F. oxysporum* (Figure 1b).

To investigate the subcellular location of UvCYP503, a UvCYP503-GFP fusion construct was created and inserted into a *UvCYP503* mutant strain in *U. virens*. UvCYP503-GFP fusion protein was shown to be localized in the cytoplasm of hyphae and conidia, as demonstrated by fluorescence detection (Figure 1f).

UvCYP503 positively regulates the mycelial growth and spore production of U. virens

We used the homologous recombination technique to knocked out the *UvCYP503* gene in *U. virens*. A *hygromycin resistance gene cassette* was inserted in place of the *UvCYP503* gene in the wild-type *U. virens* strain (Figure 1c). The successful replacement was confirmed by southern blot experiment. Δ*Uvcyp503*-104 and Δ*Uvcyp503*-107 were verified to be the appropriate knockout mutants when the target band measured 6.3 kb in the wild-type strain became 3.8 kb in the knockout strain (Figure 1d). For complemented strain Δ*Uvcyp503*-C, a vector containing a complete copy of the *UvCYP503* gene was introduced into the deletion mutant. RT-qPCR analysis confirmed successful backfilling of *UvCYP503* expression in the Δ*Uvcyp503*-C strain (Figure 1e). After incubating on PSA medium for 14 days, culture studies revealed that Δ*Uvcyp503* mutants had significantly smaller colony diameters than the wild-type strain. On the other hand, Δ*Uvcyp503*-C strain exhibited morphology that was akin to the wild-type strain, suggesting that Δ*Uvcyp503*-C had successfully restored *UvCYP503* (Figure 2a,b). Additionally, the Δ*Uvcyp503* mutants' spore production were found to be four-times less than that observed in both the wild-type and complemented strains after seven days of growth in PS medium (Figure 2c,d). These findings suggested that *UvCYP503* positively regulates the growth and spore production of *U. virens*.

UvCYP503 positively regulates pathogenesis in U. virens

To assess the effect of *UvCYP503* gene on the virulence of *U. virens*, spore and mycelia mixtures of the wild-type, Δ*Uvcyp503*-104, Δ*Uvcyp503*-107, and Δ*Uvcyp503*-

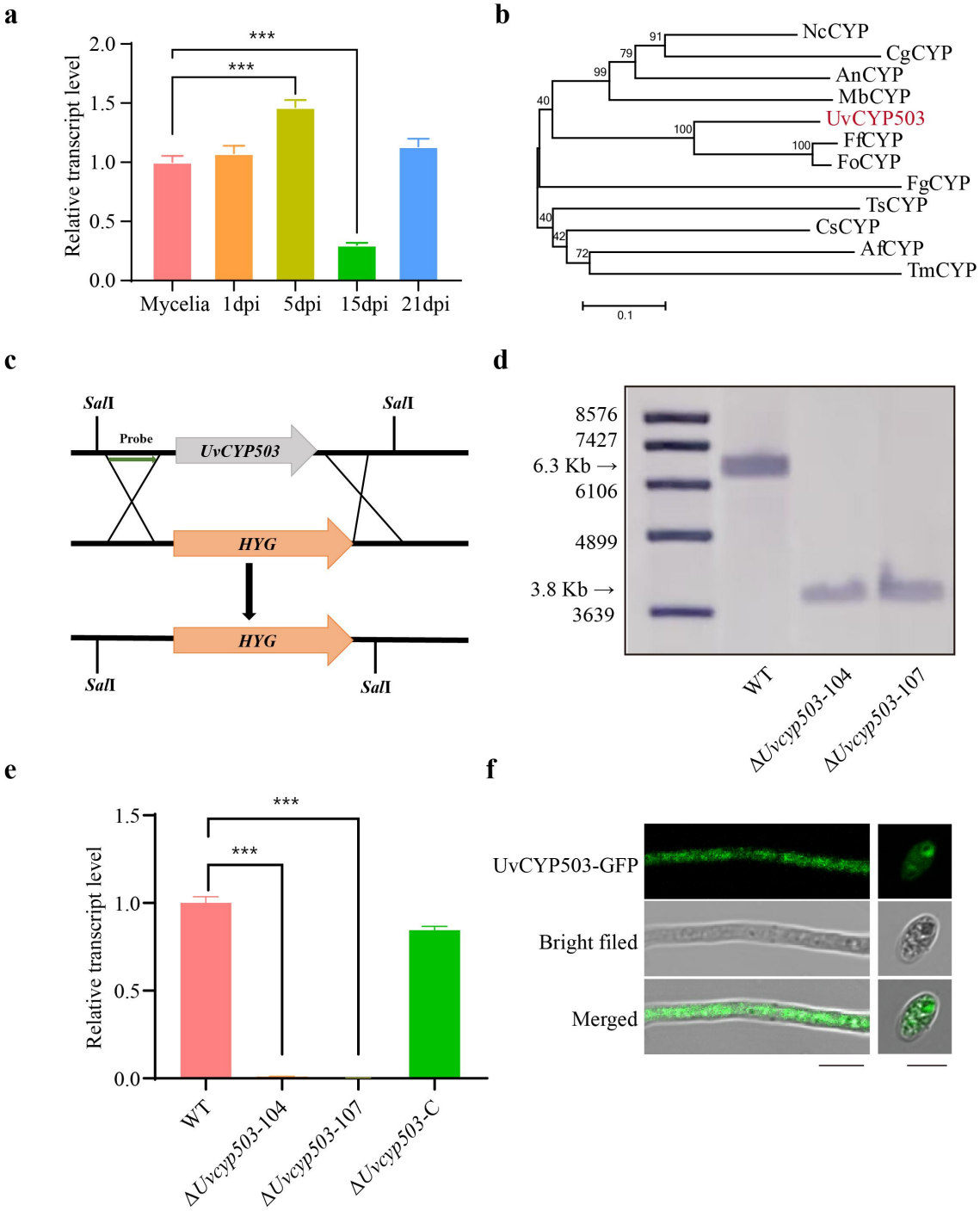

Figure 1. Identification of CYP503. a, RT-qPCR showed the expression patterns of *UvCYP503* during *U. virens* infection. Compared to the mycelial stage, notable upregulation of *UvCYP503* expression was observed at 5 dpi. b, Phylogenetic analysis of UvCYP503 homologous from various fungi, including *Neurospora crassa* (XP_963189.1), *Chaetomium globosum* (XP_001227319.1), *Aspergillus niger* (KAI3075406.1), *Metarhizium brunneum* (QLI74119.1), *Fusarium fujikuroi* (QGI65211.1), *F. oxysporum* (EWY92039.1), *F. graminearum* (WXC64557.1), *Talaromyces stipitatus* (XP_002486599.1), *Colletotrichum siamense* (KAF4880297.1), *A. flavus* (XP_041151326.1), and *T. marneffei* (EEA24836.1). c, Strategy outline for knockout *UvCYP503* and targeted locations for *Sal*I restriction enzyme application. *HYG*, *Hygromycin resistance gene cassette*. d, Southern blot examination was conducted on wild-type and *UvCYP503* knockout strains. Genomic DNA from these strains was fragmented using *Sal*I enzyme and then analysed through southern blotting, employing a probe positioned upstream of the *UvCYP503* coding sequence (depicted by the green arrow in figure 2c). Δ*Uvcyp503*-104 and Δ*Uvcyp503*-107 were verified to be the appropriate knockout mutants. e, RT-qPCR analysis confirmed successful complementation of *UvCYP503* expression in the Δ*Uvcyp503*-C strain. The *β-tubulin* gene was used as an internal standard, and applying the $2^{-\Delta\Delta CT}$ method, relative gene expression levels were determined. The mean ± SEM was calculated using three biological replicates. Statistical significance was determined based on the outcomes of the Student's *t*-test. To indicate varying levels of statistical significance, the symbols *, **, and *** were employed, correspondingly representing $p < 0.05$, $p < 0.01$, and $p < 0.001$. f, UvCYP503-GFP fusion protein localizes in the cytoplasm of hyphae and conidia, as demonstrated by fluorescence detection. Scale bar = 5 μm.

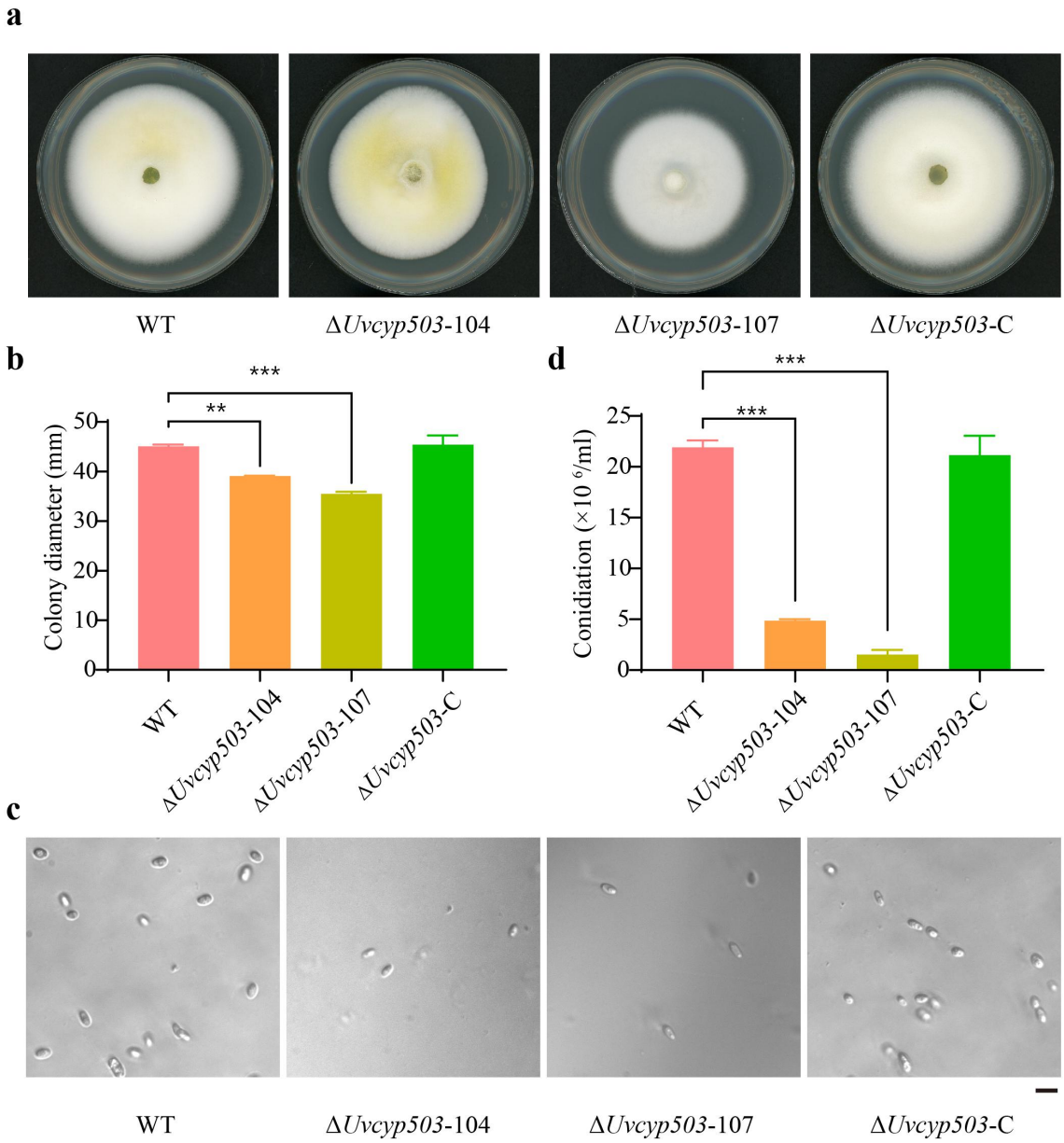

Figure 2. *UvCYP50* positively regulates the mycelial growth and spore production of *U. virens*. a, the colony of each strain after incubating on PSA medium for 14 days. b, Δ*Uvcyp503* mutants had significantly smaller colony diameters than the wild-type strain. Mycelium diameter of the wild-type, Δ*Uvcyp503*-104, Δ*Uvcyp503*-107, and complemented strain on the PSA medium was measured after 14 days at 28°C. Results are depicted as the mean ± SEM from three separate replicates. Significant differences, marked with asterisks, were identified using a Student's *t*-test, with *p*-values less than 0.001 (denoted as ***) and *p*-values less than 0.01 (denoted as **). c, Spores production of the Δ*Uvcyp503* mutants was found to be four-times less than that observed in both the wild-type and complemented strains after seven days of growth in PS medium. d, Spores of each strain were photographed under microscope. Scale bar = 10 μm.

C strains were injected into the panicles of Wanxian98 rice plants. We counted the false smut balls on each infected panicle after 21 days. Statistics revealed that spikes injected with the complemented and wild-type strains had significantly more false smut balls than spikes inoculated with the mutant strains. The number of false smut balls on spikes injected with the wild-type and complemented strains was comparable (Figure 3a, b). This finding indicates that *UvCYP503* positively regulates *U. virens* pathogenicity.

UvCYP503 affects the transcription of pathogenicity-related genes

We performed an RNA-seq analysis to look into the intrinsic mechanism by which *UvCYP503* influences the

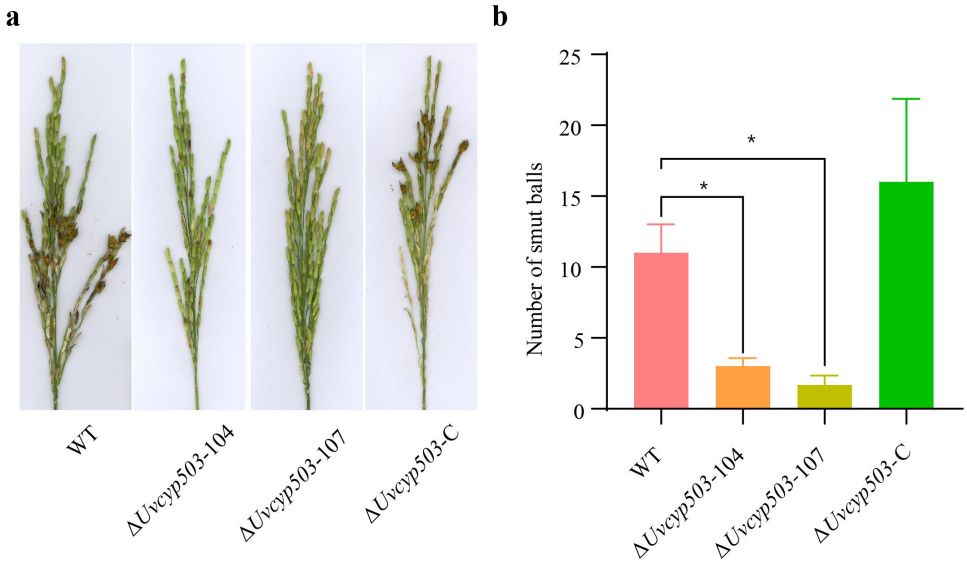

Figure 3. *UvCYP503* positively regulates pathogenesis in *U. virens*. a, the false smut balls on spikes at 21 days post inoculated with indicated strain. b, statistics revealed that spikes injected with the complemented and wild-type strains had significantly more false smut balls than spikes inoculated with the mutant strains. the results are reported as the mean ± SEM from three separate experiments. Asterisks (*) signify statistically significant differences with a *p*-value less than 0.05, as assessed by the Student's *t*-test.

pathogenicity of *U. virens*. Data indicated that 381 genes exhibited increased expression, while 213 genes showed decreased expression among the 594 genes that showed differential expression in the *UvCYP503* mutant relative to the wild-type strain (Figure 4a). Functional categorization of differentially expressed genes (DEGs) was achieved through Gene Ontology (GO) enrichment analysis (Figure 4b). Data demonstrated that DEGs were significant in enrichment in oxidoreductase activity, transmembrane transport and other categories. Furthermore, the Kyoto Encyclopedia of Genes and Genomes (KEGG) analysis highlighted significant enrichment of pathways across three categories: metabolism, environmental information processing, and organismal systems (Figure 4c). It was discovered that the genes ranking in the top 30 of the KEGG analysis are essential for many biological processes, such as metabolic pathways, biosynthesis of secondary metabolites, and others (Figure 4d).

UvPr1a, *UvPal1*, and *UvSTE50* genes, which positively regulate the pathogenicity of *U. virens* [36–38], were significantly down-regulated in the Δ*Uvcyp503* mutant according to RT-qPCR data (Figure 5a). To comprehensively understand the transcription of *CYP450* genes in the Δ*Uvcyp503* mutant, a heat map was constructed using transcriptome data, showing that many *CYP450* genes were down-regulated in the Δ*Uvcyp503* mutant (Figure 5b). These findings indicate that *UvCYP503* regulates the expression of genes linked to pathogenesis and *CYP450*, aligning with the observed decrease in virulence of the Δ*Uvcyp503* mutant strain.

UvCYP503 regulates the transcription of genes related to various stress responses

Based on the RNA-seq analysis and RT-qPCR assay data, deletion of *UvCYP503* significantly impacted the expression of genes associated to stress response. The reported genes *UvHOG1*, *UvPDEH*, and *UvSUN1*, which positively regulate *U. virens* response to cell wall stress, showed decrease expression in the Δ*Uvcyp503* mutant (Figure 6a) [39–41]. *UvCom1*, *UvCCHC3*, and *UvCCHC4* genes, which negatively regulate responses to oxidative stress, showed decreased expression in the Δ*Uvcyp503* mutant (Figure 6b) [42,43]. Similarly, *UvPmk1*, *UvCDC2*, and *UvCCHC6*, which negatively regulate responses to hyperosmotic stress, were decreased in the Δ*Uvcyp503* mutant (Figure 6c) [43,44]. Therefore, we examined the responses of each strain to cell wall, oxidative, and hyperosmotic stresses by measuring the inhibition rates of growth on PSA media supplemented with 0.03% SDS, 0.05% H_2O_2, and 0.9 M sorbitol (Figure 6d). When grown in SDS-containing medium, the Δ*Uvcyp503* mutants displayed notably higher inhibition rates compared to both the wild-type and complemented strains. Conversely, in H_2O_2 and sorbitol-supplemented medium, the Δ*Uvcyp503* mutants exhibited significantly lower inhibition rates compared to the wild-type and complemented counterparts (Figure 6e). These findings suggested that an association between *UvCYP503* and cell wall integrity, oxidative tolerance, and osmoregulation.

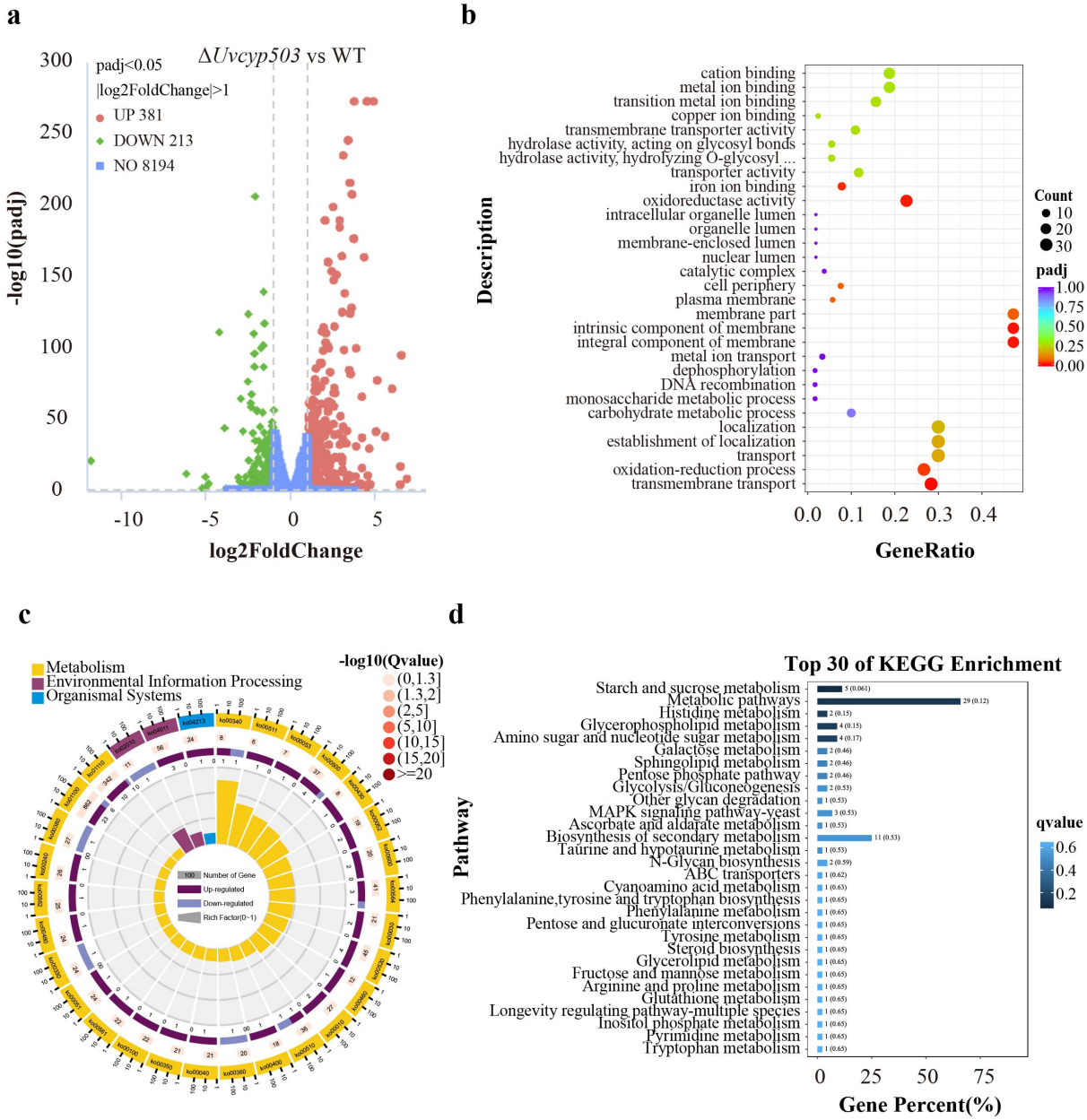

Figure 4. Comparative transcriptomic analysis of the WT and *Δ Uvcyp503 strain*. a, Differentially expressed genes (DEGs) (Δ*Uvcyp503* vs. wild-type) are presented by volcano plot. Compared to the wild-type strain, 594 genes exhibited differential expression in the Δ*Uvcyp503* strain, with 381 genes up-regulated and 213 down-regulated (adjusted *p*-value ≤0.05, $\log_2$FoldChange ≥1). b, All DEGs showed significant enrichment in oxidoreductase activity, oxidation-reduction process, transmembrane transport terms, among others. c, KEGG analysis suggested that the enriched pathways fell into three categories: metabolism, environmental information processing, and organismal systems. d, the genes ranking in the top 30 of the KEGG analysis are essential for many biological processes, such as metabolic pathways, biosynthesis of secondary metabolites, and others.

UvCYP503 is essential for sensitivity to azole fungicides

The UvCYP51 protein has been reported to have high affinity with tebuconazole, leading to sensitivity to this compound [45,46]. The heat map showed decreased transcription of *UvCYP51* (*Uv8b_02646*) in the Δ*Uvcyp503* mutant (Figure 5b). For further investigate the role of the *UvCYP503* gene in the response to azole fungicides, we have cultured each strain on PSA and PSA medium treated with 1 mg/L difenoconazole or 0.05 mg/L tebuconazole (Figure 7a,c). Under these two azole fungicides treated, the Δ*Uvcyp503* mutants exhibited significantly lower inhibition rates compared to the wild-type and complemented strains (Figure 7b,d), indicating that *UvCYP503* is crucial for azole fungicides sensitivity.

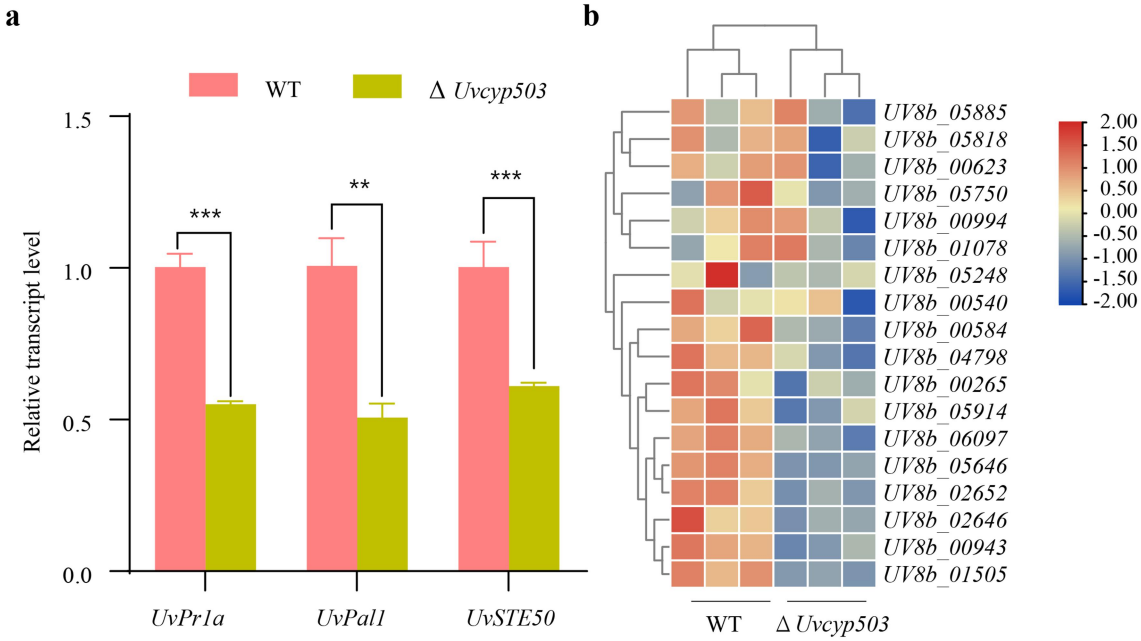

Figure 5. *UvCYP503* affects the transcription of pathogenesis-related genes. a, the relative transcriptional level of pathogenesis-related genes *UvPr1a*, *UvPal1*, and *UvSTE50* in the Δ*Uvcyp503* mutant were significantly decreased compared to the wild-type, as determined by RT-qPCR using the *β-tubulin* gene as a control and the $2^{-\Delta\Delta CT}$ calculation method, the findings are presented as the average value ± SEM from three separate replicates. The triple asterisks (***) signify a *p*-value less than 0.001, and double asterisks (**) denote a *p*-value less than 0.01, as evaluated through the Student's *t*-test. b, Some *CYP450* genes were down-regulated in Δ*Uvcyp503* mutant compared with those of in wild-type.

Discussion

Rice false smut is one of the most serious diseases threatening rice production and food safety in the world by causing smut balls and mycotoxin production [47]. *CYP450* genes are involved in many aspects of an organism's life activities. We investigated the biological role of the CYP450 family gene *CYP503* in *U. virens* in this study and discovered that it positively influences pathogenicity, spore formation, and growth. Furthermore, RNA-seq data revealed that CYP503 regulates the transcription of genes associated with pathogenicity and also influences the expression of other *CYP450* genes, thereby affecting pathogenicity and sensitivity to azole fungicides.

The *CYP450* genes are involved in fungal pathogenicity [26,48,49]. The deletion of *CYP450* genes (*DFg03700*, *DFg02111*, *DFg00012*, *DFg10451*, and *DFg12737*) in *F. graminearum* resulted in weakened growth and sporulation abilities, as well as decreased pathogenicity [24]. In our study, we observed that the Δ*Uvcyp503* mutants had weakened growth and sporulation abilities. A cytochrome *P450* gene in *Moniliophthora perniciosa* showed significantly higher expression at 48 and 72 hours post inoculation [50]. When *MoMCP1* is knocked out in *M. oryzae*, other genes relevant to pathogenicity are affected differently [25]. Similarly, we discovered that *UvCYP503* expression was elevated at 5 dpi. Our virulence inoculation experiment also demonstrated that knocking out *UvCYP503* reduced the pathogenicity of *U. virens*, and *UvCYP503* knockout significantly decreased the expression of pathogenesis-related genes, including *UvPr1a*, *UvPal1*, and *UvSTE50*. These results indicate that the *UvCYP503* gene plays a significant role in promoting *U. virens* infection in rice.

Previous studies have shown that the alteration of stress-related genes in *U. virens* is linked to its virulence. For example, the cAMP pathway gene *UvPDEH* knockout results in increased sensitivity to cell wall stress, decreased development, and virulence [40]. *Uvsun1* knockout leads to decreased cell wall integrity, also decrease the hyphal growth, conidiation, and virulence [41]. In this study, these genes showed significantly decreased expression in the Δ*Uvcyp503* strain compared with wild-type strain. Phenotypic experiment on petri dishes confirmed that *UvCYP503* participates in the regulation of cell wall stress. This suggests that the reduced pathogenicity of the Δ*Uvcyp503* mutants may be caused by increased sensitivity to cell wall stress.

Because the CYP450 protein CYP51 mediates a crucial step in the ergosterol synthesis pathway, it makes CYP51 a

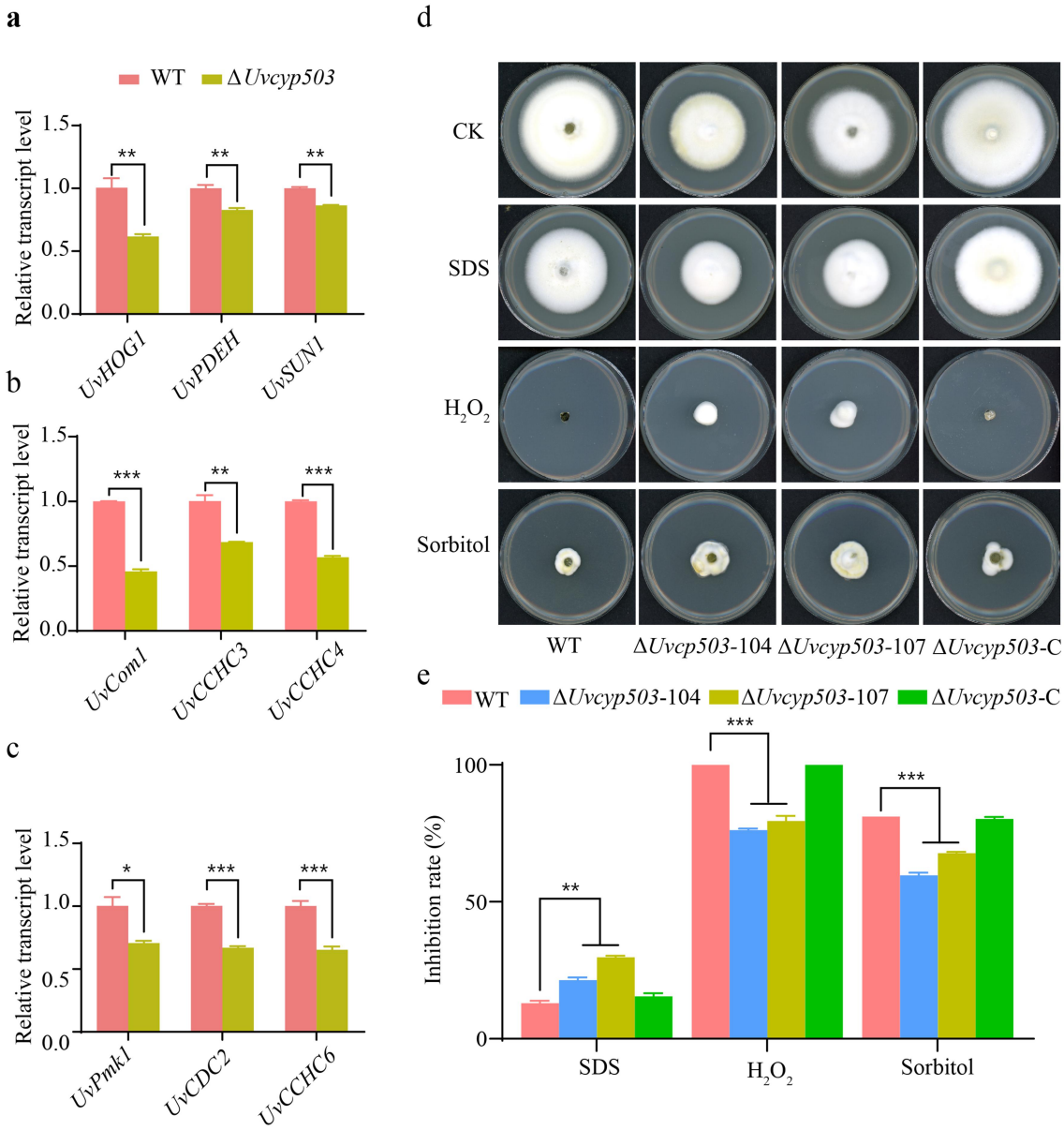

Figure 6. *UvCYP503* regulates the transcription of genes related to various stress responses. a–c, the relative transcriptional level of genes responding to cell wall stress (a), oxidative stress (b), hyperosmotic stress (c) showed decreased expression in the Δ*Uvcyp503* mutant. d, Colony morphologies of wild-type, Δ*Uvcyp503*-104, Δ*Uvcyp503*-107, and complemented strains were analysed by inoculating mycelial plugs on PSA plates and PSA supplemented with 0.03% SDS, 0.05% H_2O_2, or 0.9 M Sorbitol at 28°C for 14 days. CK, control. e, Quantitative date of indicated strains in response to various stress responses. On the sds-containing medium, the Δ*Uvcyp503* mutants displayed notably higher inhibition rates compared to both the wild-type and complemented strains. In contrast, on H_2O_2 and sorbitol-supplemented medium, the Δ*Uvcyp503* mutants exhibited significantly lower inhibition rates than their wild-type and complemented counterparts. The presented data represent the average with standard error of the mean (SEM) from three separate experiments. Statistically significant differences are marked with asterisks, corresponding to *p*-values of less than 0.001 (***), 0.01 (**), or 0.05 (*) as determined by the Student's *t*-test.

target for azole antifungal drugs. Currently, many azole fungicides are used in agriculture [46]. In our study, the Δ*Uvcyp503* strain showed decreased expression of *CYP51* in contrast to the wild-type strain. In the previous study, mutations in the Y137H site of *VvCYP51* reduced *Villosiclava viren*'s sensitivity to tebuconazole [45]. A point mutation at G54 of the Cyp51A protein of *As. fumigatusis* is related to itraconazole resistance [51]. Our phenotypic experiment on petri dishes showed that the Δ*Uvcyp503* mutants are more resistant to azole fungicides. This suggests that knockout of the *CYP503* gene leads to fungal resistance to azoles, raising the possibility that CYP503 could be a target for azole antifungal drug development in *U. virens*.

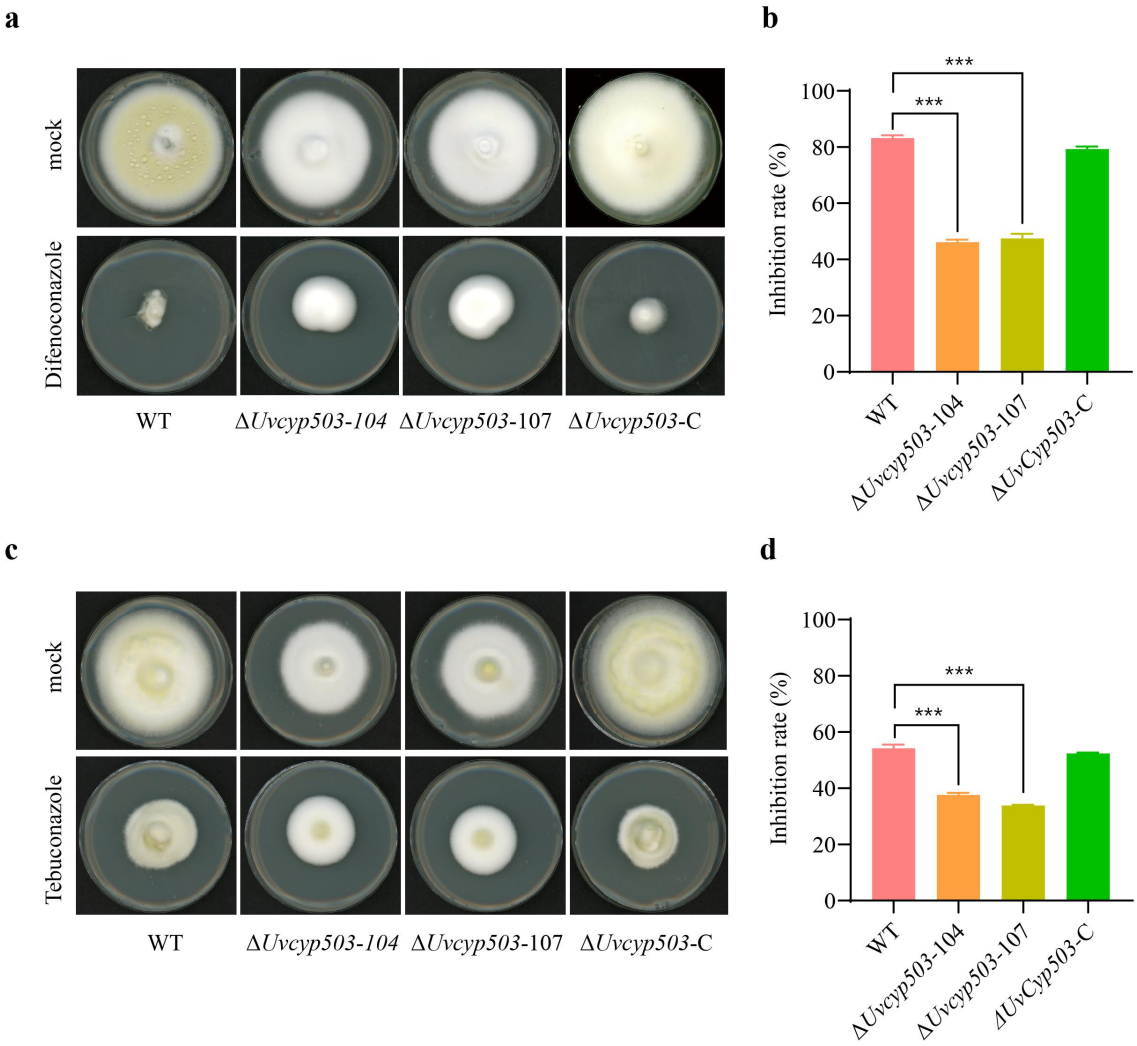

Figure 7. *UvCYP503* is involved in the sensitivity to azole fungicides. Mycelial growth of each strain on PSA medium or with 1 mg/mL difenoconazole (a) and 0.05 mg/mL tebuconazole. (c). The inhibition rates of wild-type, Δ*Uvcyp503* mutants, and complemented strains treated with 1 mg/L difenoconazole (b) and 0.05 mg/mL tebuconazole (d). The Δ*Uvcyp503* mutants exhibited significantly lower inhibition rates to difenoconazole and tebuconazole compared to the wild-type and complemented strains. The outcomes are presented as the average with standard error of the mean (SEM) based on three replicates. Asterisks (***) signify statistically significant differences at a *p*-value of less than 0.001, as determined by a Student's *t*-test.

Overall, our work sheds important light on the functional characterization of *UvCYP503* and its involvement in fungal growth, sporulation, pathogenicity, stress response, and sensitivity to azole fungicides. This study contributes to a better understanding of the mechanisms underlying the *U. virens* pathogenic process and may trigger more research on azole fungicides for improved management of plant diseases caused by *U. virens*. Further studies are necessary to determine the *CYP450*-mediated signalling molecules and clarify the molecular processes underlying the fungal infection process.

Material and methods

Culture conditions for strains cultivation and spore production

In conducting the mycelial growth experiment, we cultivated each strain in PSA medium at 28°C for a duration of 14 days. The PSA medium was formulated using 200 grams per litre of potato, 20 grams per litre of sucrose, and 20 grams per litre of agar, subsequently sterilized at 121°C for 20 minutes. Spore production experiments were conducted on PS medium. The PS medium was prepared by combining 200 grams per

litre of potato and 20 grams per litre of sucrose, followed by sterilization at 121°C for 20 minutes. Six mycelial agar plugs (diameter 5 mm) obtained from 14-days colonies of each strain, were shaken in 50 millilitres of PS medium at a rate of 160 revolutions per minute for seven days at 28°C in the dark. Each strain's spore suspensions were dropped onto a haemocytometer plate for counting and then photographed under a microscope. Three separate biological experiments were conducted, with three duplicates for each.

UvCYP503 gene analysis and construction of ΔUvcyp503 and complemented strains

The NCBI website (https://www.ncbi.nlm.nih.gov/) provided the sequences of gene and protein. Phylogenetic studies were performed using MEGA 6.0 and the neighbour-joining algorithm technique [52]. The *UvCYP503* (*Uv8b_06095*) sequence was acquired from the NCBI database. We amplified the upstream (878 bp) and downstream (849 bp) flanking sequences of the *UvCYP503* gene from the genomic DNA of *U. virens* wild-type strain JS60–2 (Kindly provide by Chaoxi Luo of Huazhong Agricultural University, Wuhan, China) in order to create the *Uvcyp503* deletion mutant Δ*Uvcyp503*. These fragments were cloned into the vector *pFGL821* (Addgene 58,223) and then introduced into the spores of JS60–2 using the ATMT technique as described by Yu's protocol [53]. The promoter region (1909 bp), along with coding sequence, and 3′-untranslated region (599 bp) sections of *UvCYP503* were amplified from the genomic DNA of the JS60–2 strain then inserted into vector pFGL823 for the complementation experiment [33]. Through the ATMT method, the plasmid was inserted into the Δ*Uvcyp503* mutant. Southern blot tests, RT-qPCR analysis, and PCR were used to verify the transformants. Supplementary Table S1 has a list of the amplification primers.

Southern experimental test

We extracted genomic DNA from the wild-type strain and Δ*Uvcyp503* mutants using phenol/chloroform to remove residual protein. This DNA wAS digested with *Sal*I for 12 hours, and then bands of different sizes were separated using 0.8% agarose gel electrophoresis. We blotted the gel by capillary transfer with 10 × SSC onto a positively charged nylon membrane. UV crosslinking was a method we used to fix DNA on the membrane. An upstream fragment of *UvCYP503* was extracted to be used as a probe, labelled with digoxigenin-dUTP for 20 hours at 37° C. Hybridization was carried out following the Meng's protocol [33].

RNA isolation and RT-qPCR analysis

Mycelia from each strain were collected and powdered using liquid nitrogen. Trizol reagent (Cat. No. B511311, Sangon Biotech, China) was used to extract RNA. Utilizing the *β-tubulin* gene as an internal standard, RT-qPCR was carried out. Applying the $2^{-\Delta\Delta CT}$ technique, relative gene expression levels were computed. The mean ± SEM was calculated from three biological replicates. *P*-values were generated using the results of the student's *t*-test. The symbols *, **, and *** are utilized to signify statistical significance at $p < 0.05$, $p < 0.01$, and $p < 0.001$ levels, respectively. The primer pairs of genes *UvCYP503*, *UvPr1a*, *UvPal1*, *UvSTE50*, *UvHOG1*, *UvPDEH*, *UvSUN1*, *UvCom1*, *UvCCHC3*, *UvCCHC4*, *UvPmk1*, *UvCDC2*, and *UvCCHC6* are in Table S1.

The same method as above was used to ascertain the relative expression of *UvCYP503* during infection, RNA was isolated from rice spikelets infected with the wild-type strain. The rice spikelets had been collected at 0, 1, 5, 15, and 21 dpi. The RT-qPCR analysis primers are listed in table S1.

Subcellular localization of UvCYP503-GFP and image processing

The GFP tag of the *pFGL823-GFP-TrpC* vector was fused to the C-terminus of UvCYP503, which allowed us to observe the subcellular localization of UvCYP503. The Δ*Uvcyp503* strain was transformed with this plasmid using ATMT. Photographs and observations of UvCYP503-GFP localization were taken with a Confocal Laser Scanning Microscope 980 (ZEISS LSM980). Images were processed using ImageJ software.

Pathogenicity assay

Artificial inoculation was performed in a greenhouse setting. Mycelium from each strain was shaken in PS medium for 7 days to produce liquid cultures of mycelia and spores, which were then homogenized in a blender. Using PS medium, the spore density was adjusted to 1×10^6 conidia per millilitre. The inoculum was applied to rice cultivar Wanxian98 (*Oryza sativa L. indica*) panicles (5–7 days before heading) by injecting liquid cultures from the side until overflowing using syringes. The temperature was first maintained at 22°C for the first 2 days with water sprayed every 3 hours and shading applied. Subsequently, the temperature was

increased to 28°C with humidity above 70% and a 12 hours photoperiod. We numbered and took pictures of each panicle's false smut balls at 21 dpi. This experiment was repeated three times.

Abiotic stress response analysis

The wild-type, Δ*Uvcyp503*-104, Δ*Uvcyp503*-107, and Δ*Uvcyp503*-C strains were grown on PSA media supplemented with 0.03% SDS, 0.05% H_2O_2, 0.9 M Sorbitol at 28°C. Colony diameters were measured after 14 days. The formula used to compute the inhibition rates was according to Meng's article [33]. Every experiment was run three times, each with three replicates.

Evaluating the responsiveness of *U. virens* strains to azole fungicides

The fungicides were dissolved in DMSO and diluted in PSA. Each strain was inoculated at the middle of PSA plates and PSA containing 1 mg/mL Difenoconazole (Cat. No. HY-B0850, MCE, USA), or 0.05 mg/l tebuconazole (Cat. No. HY-B0852, MCE, USA). Three replicates were carried out for each treatment. Results were recorded as photographs and inhibition rates were calculated using the formula for abiotic stress response analysis after incubation at 28°C for 14 days [46]. Experiments were repeated three times.

RNA-seq experiment

For RNA-seq analysis, mycelia of the JS60–2 strain and the Δ*Uvcyp503* strain were collected after culture in PS medium for 6 days. Total RNA was extracted, and RNA quality was assessed using the Agilent 5400 bioanalyzer. Library construction followed the methods described by Parkhomchuk [54], subsequently undergoing sequencing RNA-seq data commenced with clean data, derived through rigorous quality control of raw data. Three independent biological replicates were performed. Reference genome and gene annotation files were procured from the NCBI website. Genes classified as differentially expressed were those screened by DESeq2 with an adjusted $|\log_2(\text{FoldChange})| \geq 1$ and $\text{Padj} \leq 0.05$ (Table S2) [33]. GO enrichment analysis was conducted on these differentially expressed genes using the cluster Profiler *R* package [55], the GO terms with a corrected padj ≤0.05 were considered significantly enriched, providing valuable insights into functional categorization. KEGG pathways analysis was performed on the GENE DENOVO website (https://www.omicshare.com/tools/Home/Soft/pathwaygseasenior). The *p*-value was corrected by FDR to get *q*-value, following a criterion of *q*-value ≤0.05, and pathways meeting this requirement were identified as significantly enriched with differentially expressed genes.

Data availability statement

The RNA-seq analysis data that support the findings of this study are available with accession number: SRR30760091-SRR30760096 in NCBI. The source data of this study are available in figshare with doi number 10.6084/m9.figshare.27132246 (https://doi.org/10.6084/m9.figshare.27132246).

Author contributions

Xiuxiu Cao: Data curation, Formal analysis, Investigation, Validation, Visualization. Writing-original draft; Hui Wen: Data curation, Resources; Dagang Tian: Supervision; Huanbin Shi: Formal analysis, Methodology, Supervision, Software, Visualization; Kabin Xie: Supervision; Jiehua Qiu: Conceptualization, Funding acquisition, Methodology, Project administration, Resources, Supervision, Writing-review & editing; Yanjun Kou: Conceptualization, Funding acquisition, Methodology, Project administration, Resources, Supervision, Writing-review & editing; All the authors have read and approved the manuscript.

Disclosure statement

No potential conflict of interest was reported by the author(s).

Funding

This research was funded by the Zhejiang Provincial Natural Science Foundation of China [LZ23C130002 and LR24C140001], the National Natural Science Foundation of China; external cooperation projects of FAAS [DWHZ2024–07], Zhejiang Science and Technology Major Program on Rice New Variety Breeding, [2021C02063–3], Central Public-interest Scientific Institution Basal Research Fund of China National Rice Research Institute [CPSIBRF-CNRRI-202116], and Innovation Program of Chinese Academy of Agricultural Sciences [Y2023QC22 and CAAS-CSCB-202301]; the Joint Open Competitive Project of the Yazhou Bay Seed Laboratory and China National Seed Company Limited [B23YQ1514 and B23CQ15EP], the National Natural Science Foundation of China; external cooperation projects of FAAS [DWHZ2024–07].

ORCID

Xiuxiu Cao http://orcid.org/0000-0003-2991-663X
Jiehua Qiu http://orcid.org/0000-0002-6990-7247
Yanjun Kou http://orcid.org/0000-0003-4189-0962

References

[1] Kelly SL, Lamb DC, Jackson CJ, et al. The biodiversity of microbial cytochromes P450. Adv Microb Physiol. 2003;47:131–186. doi: 10.1016/s0065-2911(03)47003-3

[2] Kelly SL, Kelly DE. Microbial cytochromes P450: biodiversity and biotechnology. Where do cytochromes P450 come from, what do they do and what can they do for us? Philos Trans R Soc Lond B Biol Sci. 2013;368 (1612):20120476. doi: 10.1098/rstb.2012.0476

[3] Cresnar B, Petric S. Cytochrome P450 enzymes in the fungal kingdom. Biochim Biophys Acta. 2011;1814 (1):29–35. doi: 10.1016/j.bbapap.2010.06.020

[4] Durairaj P, Malla S, Nadarajan SP, et al. Fungal cytochrome P450 monooxygenases of *Fusarium oxysporum* for the synthesis of ω-hydroxy fatty acids in engineered *Saccharomyces cerevisiae*. Microb Cell Fact. 2015;14 (1):45. doi: 10.1186/s12934-015-0228-2

[5] Durairaj P, Hur JS, Yun H. Versatile biocatalysis of fungal cytochrome P450 monooxygenases. Microb Cell Fact. 2016;15(1):125. doi: 10.1186/s12934-016-0523-6

[6] Wang L, Wu X, Gao C, et al. A fungal P450 enzyme from *Fusarium graminearum* with unique 12β-steroid hydroxylation activity. Appl Environ Microbiol. 2023;89(3):e0196322. doi: 10.1128/aem.01963-22

[7] Ferrer-Sevillano F, Fernández-Cañón JM. Novel *phacB*-encoded cytochrome P450 monooxygenase from *Aspergillus nidulans* with 3-hydroxyphenylacetate 6-hydroxylase and 3,4-dihydroxyphenylacetate 6-hydroxylase activities. Eukaryot Cell. 2007;6(3):514–520. doi: 10.1128/EC.00226-06

[8] Ning D, Wang H, Ding C, et al. Novel evidence of cytochrome P450-catalyzed oxidation of phenanthrene in *Phanerochaete chrysosporium* under ligninolytic conditions. Biodegradation. 2010;21(6):889–901. doi: 10.1007/s10532-010-9349-9

[9] Zhang S, Widemann E, Bernard G, et al. CYP52X1, representing new cytochrome P450 subfamily, displays fatty acid hydroxylase activity and contributes to virulence and growth on insect cuticular substrates in entomopathogenic fungus *Beauveria bassiana*. J Biol Chem. 2012;287 (16):13477–13486. doi: 10.1074/jbc.M111.338947

[10] Lin L, Fang W, Liao X, et al. The *MrCYP52* cytochrome P450 monoxygenase gene of *Metarhizium robertsii* is important for utilizing insect epicuticular hydrocarbons. PLOS ONE. 2011;6(12):e28984. doi: 10.1371/journal.pone.0028984

[11] George HL, VanEtten HD. Characterization of pisatin-inducible cytochrome p450s in fungal pathogens of pea that detoxify the pea phytoalexin pisatin. Fungal Genet Biol. 2001;33(1):37–48. doi: 10.1006/fgbi.2001.1270

[12] Tudzynski B, Hedden P, Carrera E, et al. The *P450–4* gene of *Gibberella fujikuroi* encodes *ent*-kaurene oxidase in the gibberellin biosynthesis pathway. Appl Environ Microbiol. 2001;67(8):3514–3522. doi: 10.1128/AEM.67.8.3514-3522.2001

[13] Tudzynski B, Rojas MC, Gaskin P, et al. The gibberellin 20-oxidase of *Gibberella fujikuroi* is a multifunctional monooxygenase. J Biol Chem. 2002;277(24):21246–21253. doi: 10.1074/jbc.M201651200

[14] Teoh KH, Polichuk DR, Reed DW, et al. *Artemisia annua* L. (Asteraceae) trichome-specific cDNAs reveal CYP71AV1, a cytochrome P450 with a key role in the biosynthesis of the antimalarial sesquiterpene lactone artemisinin. FEBS Lett. 2006;580(5):1411–1416. doi: 10.1016/j.febslet.2006.01.065

[15] Jawallapersand P, Mashele SS, Kovacic L, et al. Cytochrome P450 monooxygenase CYP53 family in fungi: comparative structural and evolutionary analysis and its role as a common alternative anti-fungal drug target. PLOS ONE. 2014;9(9):e107209. doi: 10.1371/journal.pone.0107209

[16] Zhang J, Li L, Lv Q, et al. The fungal CYP51s: their functions, structures, related drug resistance, and inhibitors. Front Microbiol. 2019;10:691. doi: 10.3389/fmicb.2019.00691

[17] Abastabar M, Hosseini T, Valadan R, et al. Novel point mutations in *cyp51A* and *cyp51B* genes associated with itraconazole and posaconazole resistance in *Aspergillus clavatus* isolates. Microb Drug Resist. 2019;25(5):652–662. doi: 10.1089/mdr.2018.0300

[18] Yakovlev IA, Hietala AM, Steffenrem A, et al. Identification and analysis of differentially expressed *Heterobasidion parviporum* genes during natural colonization of Norway spruce stems. Fungal Genet Biol. 2008;45(4):498–513. doi: 10.1016/j.fgb.2007.10.011

[19] Leal GA Jr., Albuquerque PS, Figueira A. Genes differentially expressed in *Theobroma cacao* associated with resistance to witches' broom disease caused by *Crinipellis perniciosa*. Mol Plant Pathol. 2007;8 (3):279–292. doi: 10.1111/j.1364-3703.2007.00393.x

[20] Karlsson M, Elfstrand M, Stenlid J, et al. A fungal cytochrome P450 is expressed during the interaction between the fungal pathogen *Heterobasidion annosum* sensu lato and conifer trees. DNA Seq. 2008;19(2):115–120. doi: 10.1080/10425170701447473

[21] Changenet V, Macadre C, Boutet-Mercey S, et al. Overexpression of a cytochrome P450 monooxygenase involved in orobancholbiosynthesis increases susceptibility to fusarium head blight. Front Plant Sci. 2021;12:662025. doi: 10.3389/fpls.2021.662025

[22] Minerdi D, Sadeghi SJ, Pautasso L, et al. Expression and role of CYP505A1 in pathogenicity of *Fusarium oxysporum* f. sp. Biochim Biophys Acta Proteins Proteom. 2020;1868 (1):140268. doi: 10.1016/j.bbapap.2019.140268

[23] Li W, Li P, Zhou X, et al. B_5-like heme/steroid binding domain protein, PlCB5L1, regulates mycelial growth, pathogenicity and oxidative stress tolerance in *Peronophythora litchii*. Front Plant Sci. 2021;12:783438. doi: 10.3389/fpls.2021.783438

[24] Shin JY, Bui DC, Lee Y, et al. Functional characterization of cytochrome P450 monooxygenases in the cereal head blight fungus *Fusarium graminearum*. Environ Microbiol. 2017;19(5):2053–2067. doi: 10.1111/1462-2920.13730

[25] Wang Y, Wu Q, Liu L, et al. *MoMCP1*, a cytochrome P450 gene, is required for alleviating manganese toxin revealed by transcriptomics analysis in *Magnaporthe oryzae*. Int J Mol Sci. 2019;20(7):1590. doi: 10.3390/ijms20071590

[26] Zhang D, Wang X, Chen J, et al. Identification and characterization of a pathogenicity-related gene *VdCYP1* from *Verticillium dahliae*. Sci Rep. 2016;6 (1):27979. doi: 10.1038/srep27979

[27] Sun W, Fan J, Fang A, et al. *Ustilaginoidea virens*: insights into an emerging rice pathogen. Annu Rev Phytopathol. 2020;58(1):363–385. doi: 10.1146/annurev-phyto-010820-012908

[28] Qiu J, Meng S, Deng Y, et al. *Ustilaginoidea virens*: a fungus infects rice flower and threats world rice production. Rice Sci. 2019;26(4):199–206. doi: 10.1016/j.rsci.2018.10.007

[29] Pandey N, Vaishnav R, Rajavat AS, et al. Exploring the potential of *Bacillus* for crop productivity and sustainable solution for combating rice false smut disease. Front Microbiol. 2024;15:1405090. doi: 10.3389/fmicb.2024.1405090

[30] Adhikari P. False smut of rice: a menace to rice seed production in Nepal. Cogent Food Agric. 2024;10(1). doi: 10.1080/23311932.2024.2407064

[31] Song J, Wei W, Lv B, et al. Rice false smut fungus hijacks the rice nutrients supply by blocking and mimicking the fertilization of rice ovary. Environ Microbiol. 2016;18(11):3840–3849. doi: 10.1111/1462-2920.13343

[32] Guo X, Li Y, Fan J, et al. Progress in the study of false smut disease in rice. J Agric Sci Technol. 2012;2(11):1211–1217.

[33] Meng S, Qiu J, Xiong M, et al. *UvWhi2* is required for stress response and pathogenicity in *Ustilaginoidea virens*. Rice Sci. 2022;29(1):47–54. doi: 10.1016/j.rsci.2021.12.004

[34] Tsukui T, Nagano N, Umemura M, et al. Ustiloxins, fungal cyclic peptides, are ribosomally synthesized in *Ustilaginoidea virens*. Bioinformatics. 2015;31(7):981–985. doi: 10.1093/bioinformatics/btu753

[35] Zhang Y, Zhang K, Fang A, et al. Specific adaptation of *Ustilaginoidea virens* in occupying host florets revealed by comparative and functional genomics. Nat Commun. 2014;5(1):3849. doi: 10.1038/ncomms4849

[36] Chen X, Tang J, Pei Z, et al. The 'pears and lemons' protein UvPal1 regulates development and virulence of *Ustilaginoidea virens*. Environ Microbiol. 2020;22(12):5414–5432. doi: 10.1111/1462-2920.15284

[37] Cao H, Gong H, Song T, et al. The adaptor protein UvSte50 governs fungal pathogenicity of *Ustilaginoidea virens* via the MAPK signaling pathway. J Fungi. 2022;8(9):954. doi: 10.3390/jof8090954

[38] Chen X, Li X, Duan Y, et al. A secreted fungal subtilase interferes with rice immunity via degradation of suppressor of G2 allele of *skp1*. Plant Physiol. 2022;190(2):1474–1489. doi: 10.1093/plphys/kiac334

[39] Zheng D, Wang Y, Han Y, et al. *UvHOG1* is important for hyphal growth and stress responses in the rice false smut fungus *Ustilaginoidea virens*. Sci Rep. 2016;6(1):24824. doi: 10.1038/srep24824

[40] Guo W, Gao Y, Yu Z, et al. The adenylate cyclase UvAc1 and phosphodiesterase UvPdeH control the intracellular cAMP level, development, and pathogenicity of the rice false smut fungus *Ustilaginoidea virens*. Fungal Genet Biol. 2019;129:65–73. doi: 10.1016/j.fgb.2019.04.017

[41] Yu M, Yu J, Cao H, et al. Sun-family protein *UvSUN1* regulates the development and virulence of *Ustilaginoidea virens*. Front Microbiol. 2021;12:739453. doi: 10.3389/fmicb.2021.739453

[42] Chen X, Hai D, Tang J, et al. *UvCom1* is an important regulator required for development and infection in the rice false smut fungus *ustilaginoidea virens*. Phytopathology. 2020;110(2):483–493. doi: 10.1094/PHYTO-05-19-0179-R

[43] Chen X, Pei Z, Peng L, et al. Genome-wide identification and functional characterization of CCHC-type zinc finger genes in *Ustilaginoidea virens*. J Fungi. 2021;7(11):947. doi: 10.3390/jof7110947

[44] Tang J, Bai J, Chen X, et al. Two protein kinases UvPmk1 and UvCDC2 with significant functions in conidiation, stress response and pathogenicity of rice false smut fungus *Ustilaginoidea virens*. Curr Genet. 2020;66(2):409–420. doi: 10.1007/s00294-019-01029-y

[45] Wang F, Lin Y, Yin W, et al. The Y137H mutation of *VvCYP51* gene confers the reduced sensitivity to tebuconazole in *Villosiclava virens*. Sci Rep. 2015;5(1):17575. doi: 10.1038/srep17575

[46] Liu X, Yu F, Schnabel G, et al. Paralogous *cyp51* genes in *Fusarium graminearum* mediate differential sensitivity to sterol demethylation inhibitors. Fungal Genet Biol. 2011;48(2):113–123. doi: 10.1016/j.fgb.2010.10.004

[47] Zhou L, Mubeen M, Iftikhar Y, et al. Rice false smut pathogen: implications for mycotoxin contamination, current status, and future perspectives. Front Microbiol. 2024;15:1344831. doi: 10.3389/fmicb.2024.1344831

[48] Siewers V, Viaud M, Jimenez-Teja D, et al. Functional analysis of the cytochrome P450 monooxygenase gene *bcbot1* of *Botrytis cinerea* indicates that botrydial is a strain-specific virulence factor. Mol Plant Microbe Interact. 2005;18(6):602–612. doi: 10.1094/MPMI-18-0602

[49] Takaoka S, Kurata M, Harimoto Y, et al. Complex regulation of secondary metabolism controlling pathogenicity in the phytopathogenic fungus *Alternaria alternata*. New Phytol. 2014;202(4):1297–1309. doi: 10.1111/nph.12754

[50] Leal GA, Gomes LH, Albuquerque PS, et al. Searching for *Moniliophthora perniciosa* pathogenicity genes. Fungal Biol. 2010;114(10):842–854. doi: 10.1016/j.funbio.2010.07.009

[51] Diaz-Guerra TM, Mellado E, Cuenca-Estrella M, et al. A point mutation in the 14α-sterol demethylase gene *cyp51A* contributes to itraconazole resistance in *Aspergillus fumigatus*. Antimicrob Agents Chemother. 2003;47(3):1120–1124. doi: 10.1128/AAC.47.3.1120-1124.2003

[52] Robert X, Gouet P. Deciphering key features in protein structures with the new ENDscript server. Nucleic Acids Res. 2014;42(W1):W320–W324. doi: 10.1093/nar/gku316

[53] Yu M, Yu J, Hu J, et al. Identification of pathogenicity-related genes in the rice pathogen *Ustilaginoidea virens* through random insertional mutagenesis. Fungal Genet Biol. 2015;76:10–19. doi: 10.1016/j.fgb.2015.01.004

[54] Parkhomchuk D, Borodina T, Amstislavskiy V, et al. Transcriptome analysis by strand-specific sequencing of complementary DNA. Nucleic Acids Res. 2009;37(18):e123. doi: 10.1093/nar/gkp596

[55] Ashburner M, Ball CA, Blake JA, et al. Gene ontology: tool for the unification of biology. Nat Genet. 2000;25(1):25–29. doi: 10.1038/75556